Enhanced resolution of ultra micropore size determination of biochars and activated carbons by dual gas analysis using N2 and CO2 with 2D-NLDFT adsorption models

Jacek Jagiello, Jeffrey Kenvin, Alain Celzard, Vanessa Fierro

Enhanced resolution of ultra micropore size determination of biochars and activated carbons by dual gas analysis using N_2 and CO_2 with 2D-NLDFT adsorption models

Jacek Jagiello[a*], Jeffrey Kenvin[a], Alain Celzard[b], Vanessa Fierro[b*]

[a] Micromeritics Instrument Corporation, 4356 Communications Drive, Norcross, GA 30093, United States

[b] Université de Lorraine, CNRS, IJL, F-88000 Epinal, France

[a*]Corresponding author. Tel: +1 770 624 3379. E-mail: Jacek.Jagiello@micromeritics.com

[b*]Corresponding author. Tel: +33 (0)372 749 677. E-mail: Vanessa.Fierro@univ-lorraine.fr

Abstract

In this study, biochars obtained by either direct carbonization or hydrothermal treatment of corn stems were used as precursors of two series of activated carbons (ACs). The pore size distributions (PSDs) of biochars and ACs were evaluated from N_2 and CO_2 adsorption isotherms using models based on the two-dimensional version of the non-local density functional theory (2D-NLDFT). We showed that more detailed carbon PSDs might be obtained from simultaneous (dual) gas analysis of both N_2 and CO_2 isotherms than from single isotherms. The dual gas method showed a peak at about 0.4 nm which was not detected by the single N_2 analysis. This fact is related to the restricted diffusion of N_2 into very narrow micropores at low temperatures and pressures. By modifying the lower pore width limit w_{min} in the nitrogen model, we obtained an excellent fit of the dual model to both isotherms for all studied samples, which demonstrates the reliability and robustness of this refined method. Finally, we demonstrated that this approach would allow measuring N_2 isotherms at relative pressures starting at about 0.001 rather than at 10^{-6}, which would save time without losing resolution of the calculated PSD.

2. Introduction

The word biochar is often used as a generic term referring to carbon-rich materials obtained from various bio sourced precursors submitted to thermal treatment under inert atmosphere or with limited oxygen content. Historically, biochars have been used in agriculture to improve soil fertility [1, 2]. As porous materials, biochars or their derived activated carbons (ACs) find applications in water purification processes such as removal of heavy metal ions [3-5], organic compounds [6, 7], and other pollutants [8].

Biochars are obtained by direct carbonization or by hydrothermal carbonization (HTC) of bio sourced precursors. The HTC process involves the precursor treatment at moderate temperatures and moderate self-generated pressures in an aqueous solution. Low-severity hydrothermal treatments were traditionally used to de-structure the biomass and to facilitate its decomposition or fractionation into constitutive fractions [9, 10]. HTC attracts the interest of researchers as an effective way of converting biomass into carbonaceous materials [11], which may be used as precursors of ACs obtained after further chemical or physical activation. Non-activated materials are characterized by ultra-narrow pore size distribution (PSD). Lignin-rich precursors, such as olive stones, produce carbons with textural characteristics similar to those of carbon molecular sieves [12, 13]. While those precursors

richer in cellulose and hemicellulose, such as agave, develop slightly broader PSDs [14]. HTC-derived carbons without further activation always contain a high fraction of ultramicropores (pores narrower than 0.7nm), although they also generally comprise a higher mesopore fraction than that of directly carbonized materials. The high ultramicroporous fraction is due to H_2O, CO_2, and CO evolution, acting as pore formers, during pyrolysis.

Because of the ultramicroporous character of chars, their characterization by gas adsorption methods requires particularly careful analysis of the adsorption data. In a well-known study of carbon samples obtained by carbonization of almond shells, Rodriguez-Reinoso et al. [15, 16] attributed the extremely slow adsorption of N_2 at 77 K to slow activated diffusion into fine micropores and narrow constrictions with widths similar to molecular dimeter of N_2 molecules. Since such diffusion is strongly dependent on temperature, the CO_2 adsorption at 273 K is much faster than that of N_2 at 77 K even though both molecules have similar dimeters. Based on this fact, to overcome diffusion problems of N_2 at cryogenic temperatures and to improve the analysis of carbon molecular sieves and microporous carbons, adsorption of CO_2 at 273 K was often applied [17-21]. The micropore volume of porous carbons is usually assessed by applying the Dubinin-Radushkevich (DR) equation [22] to N_2 or CO_2 adsorption isotherms.

In the present study, we characterize the nanopore structure of biochars and ACs derived from corn stigmata (CS). We use N_2 and CO_2 adsorption data measured on these materials and we apply dual gas analysis method [23] using the non-local density functional theory (NLDFT) models for adsorption of these gases on porous carbons. Similar methodology applying standard NLDFT models was described earlier [24, 25]. Here the models are based on the two-dimensional version of the theory (2D-NLDFT) for adsorption on heterogeneous carbon surfaces [23, 26, 27]. Herein, we introduced a new approach to analyze the PSD of biochars and ultramicroporous carbons in which the lower pore width limit w_{min} of the N_2 kernel is treated as an adjustable parameter. By modifying this parameter, we dramatically improved the quality of fit of the dual model to both isotherms measured on the non-activated biochars and mildly activated carbons. This parameter has a physical meaning as it provides an estimate of the minimum pore width accessible to N_2 molecules at the measurement conditions.

We show that enhanced resolution of the carbon pore structure may be obtained by using both N_2 and CO_2 adsorption isotherms than by using single isotherms, provided the new refined 2D-NLDFT model is used. Such highly detailed characterization of biochars and their

derived ACs is especially important for advanced applications such as carbon electrodes in supercapacitors [28], gas storage [19] or gas sensors [29, 30].

2. Experimental

2.1 Raw materials

Corn stigmata (CS) were obtained from Kairouan (Tunisia). The parts of corn are the tassel, leaf, stalk, and silk. Corn silk comprises the stigma and style. CS are the sticky ends of the silk where pollen attaches. CS was washed, dried and sieved as detailed elsewhere [31] prior to any kind of carbonization. CS is mainly composed of cellulose, hemicellulose and lignin (17.7, 28.9 and 28.2 %, respectively), the rest is pectin (14.1%), and wax and grease (10.9%). Concerning elemental analysis, CS has similar contents of C and O (41.9 and 41.6 wt. %, respectively), and minor amounts of H and N (5.7 and 1.5 wt. %, respectively) [31].

2.2 Activated carbon synthesis

Two series of ACs were prepared by physical activation of biochars with carbon dioxide. These biochars were obtained by two different ways:

(i) By direct carbonization of CS, carried out using 1 g of CS, which was placed at the center of a horizontal furnace equipped with a quartz tube. The tube was flushed with nitrogen at a flow rate of 100 mL/min and heated at 1°C/min up to 900°C; the final temperature was held for 1h. Cooling was carried out under nitrogen flow and the resultant sample after pyrolysis and drying at 105°C was labelled C-CS.

(ii) By hydrothermal treatment (HTC) of CS followed by carbonization described in (i). In a typical HTC experiment, 4g of CS were introduced in a glass vial containing 40g of distilled water, and the vial was put into a 200 mL Teflon-lined autoclave (Anton Parr). The autoclave was then installed for 6h in a ventilated oven pre-heated at 180°C. The choice of HTC conditions ensured total HTC conversion [32]. After HTC, carbonization and drying at 105°C, the sample was labelled CH-CS.

In order to further develop their textural properties, biochars were physically activated with CO_2 in a horizontal tubular furnace. 1g of either C-CS or CH-CS was placed in a quartz boat and transferred into a quartz tube flushed with high-purity nitrogen at a flow rate of 100 mL/min, then heated at 5°C/min up to 900°C. Once the final temperature was reached, N_2 was replaced by CO_2 at a flow rate of 60 mL/min for 0.5, 1, or 2 hours. Next, the furnace was allowed to cool under nitrogen flowing at 100 mL/min. ACs were labelled by adding the activation time in hours to the label of the biochar precursors. For example, ACs produced from C-CS by activation for 0.5 or 2 h were labelled C-CS-0.5 or C-CS-2, respectively.

3. Results and discussion

The textural properties of the carbon materials were determined from nitrogen adsorption-desorption isotherms at 77 K (Fig. 1) and carbon dioxide adsorption at 273 K, using a Micromeritics ASAP 2020 and a Micromeritics ASAP 2420, respectively. Data were treated using the MicroActive software from Micromeritics. Basic textural characteristics are collected in Table 1. The BET method was used to determine the BET area, S_{BET}, from N_2 isotherms. The DR micropore volumes $V_{DR,N2}$ and $V_{DR,CO2}$ ware determined from both nitrogen and carbon dioxide isotherms using Dubinin-Radushkevich (DR) method [22]. The total pore volume accessible by N_2 adsorption, $V_{0.97}$, was measured at a relative nitrogen pressure of 0.97.

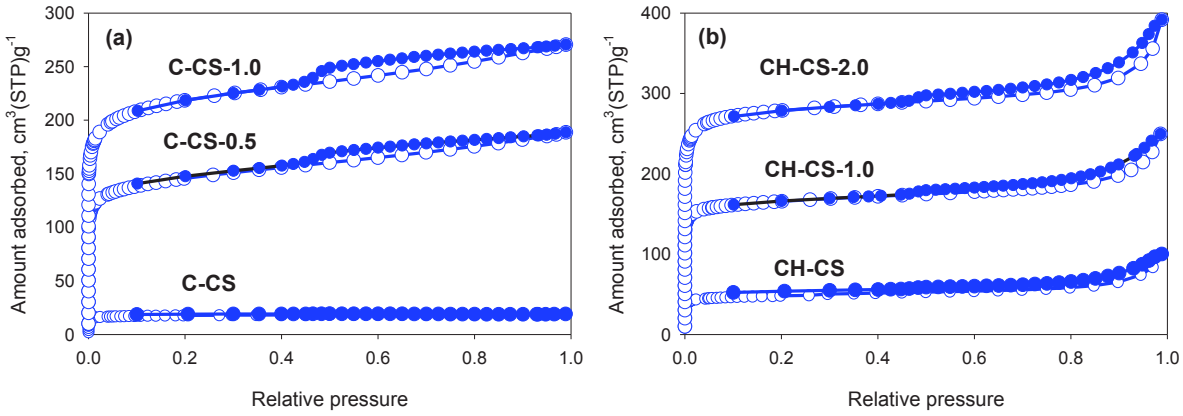

Fig. 1 – Nitrogen adsorption and desorption isotherms measured at 77 K on two carbon series C-CS (a) and CH-CS (b).

It is interesting to compare the micropore volumes evaluated using the DR method from the isotherms of CO_2 and N_2 for biochars series C-CS and CH-CS. $V_{DR,CO2}$ is significantly higher than $V_{DR,N2}$ for these biochars, which is consistent with the results reported by other authors [18, 33] indicating reduced accessibility of fine micropores to nitrogen at 77 K.

Table 1. Burn-off and basic textural characteristics of the two series of carbons.

Sample	Burn-off %	$S_{BET,N2}$ ($m^2 g^{-1}$)	$V_{DR,N2}$ ($cm^3 g^{-1}$)	$V_{DR,CO2}$ ($cm^3 g^{-1}$)	$V_{0.97}$ ($cm^3 g^{-1}$)
C-CS	75.0	47	0.02	0.14	0.03
C-CS-0.5	85.4	555	0.21	0.22	0.29
C-CS-1.0	93.2	839	0.31	0.24	0.42
CH-CS	82.9	188	0.08	0.13	0.13
CH-CS-1.0	87.9	660	0.25	0.30	0.36
CH-CS-2.0	92.7	1110	0.42	0.34	0.56

3.1 Properties of the 2D-NLDFT pore models.

A more detailed characterization of the biochars microporosity and its development due to the activation process may be obtained by the NLDFT analysis of CO_2 and N_2 isotherms using the 2D-NLDFT heterogeneous surface models [23, 26, 27] for adsorption on porous carbons. Here we apply the same models (kernels) and parameters that were developed and described earlier [23]. All PSD calculations were performed using SAIEUS software [34] available at www.nldft.com.

The earlier work was devoted to the PSD analysis of porous carbons in general. Here, we are focused on biochars and ultramicroporous carbons which require specific treatment that will be discussed in section 3.3 “Refinement of the PSD analysis”.

Like in most of the PSD calculation methods, we assume the independent pore model which by itself does not account for connectivity. It has been an attempted [35], however, to use the percolation theory in conjunction with the PSDs calculated using an independent pore model for probe molecules of different sizes to extract an estimate of the pore network. Molecular sizes of CO_2 and N_2 are quite similar, so the PSDs calculated in the present work would not be suitable for the connectivity analysis.

The parameters of the 2D-NLDFT models used in this study were derived by fitting the models to the experimental adsorption isotherms measured on the reference non-graphitized carbon black BP280 [23, 27]. It was shown [26] that N_2 isotherm of this sample is in a good agreement with the isotherms measured on the surfaces of several non-graphitized carbon blacks. Based on this fact, we regard the parameters obtained from the analysis of adsorption data measured on BP280 as representative and suitable for use in our models. It is known that the oxidation or other chemical treatments [36] may change carbon surface properties,

however, we do not consider such effects in this study. Earlier studies, based on the standard NLDFT models, by Ravikovitch at al. [37] and others [24, 38] have shown relatively good agreement between the PSDs derived from adsorption data of gases like N_2, Ar, and CO_2. This agreement encouraged us to use a combined analysis of N_2 and CO_2 in the present study.

The selected isotherms of CO_2 and N_2 kernels at 77 and 273 K were presented in the original papers [23, 27] in wide ranges of relative pressures and pore widths. Here we focus our attention to study the ultra micropore range of carbon porosity. To better understand the concept of the dual gas analysis method, we show in Fig. 2 theoretical isotherms of N_2 at 77 and CO_2 at 273 K calculated for small pores of width between 0.4 and 1.0 nm. The pores of this range fill with N_2 and CO_2 at different ranges of relative pressures. For N_2 it is between about 10^{-8} and 10^{-3}, and for CO_2 between 10^{-3} and 10^{-1} relative pressure. To analyze the width of these pores, it is necessary to measure the relevant adsorption isotherms in the relevant pressure ranges.

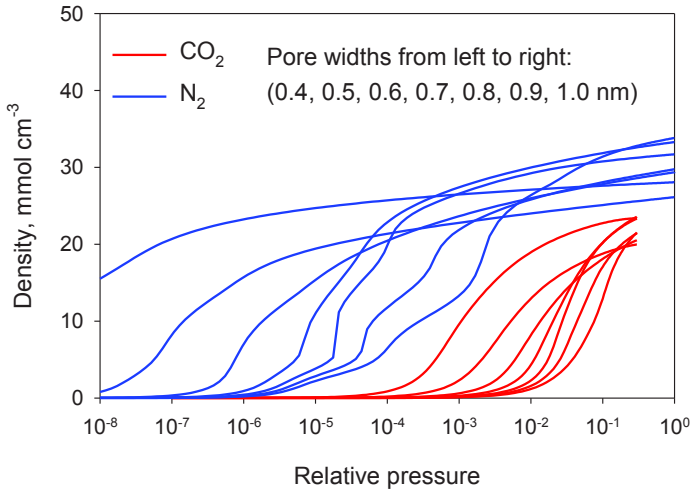

Fig. 2 – Comparison of theoretical isotherms of N_2 at 77 and CO_2 at 273 K calculated for small pores of width between 0.4 and 1.0 nm.

To illustrate the process of filling an ultramicropore, we present in Fig. 3 the density profiles of CO_2 and N_2 in the corrugated pore of width w = 0.4 nm calculated at increasing relative pressures. The curvature/corrugation of the graphene pore walls is described by a simple sine function:

$$t(x^*) = \alpha^* \sin(2\pi x^*/\lambda^*), \qquad (1)$$

where $\lambda^* = 6$ defines the periodicity and $\alpha^* = 0.45$ is the amplitude of the corrugation. Symbols with asterisk x*, λ^*, and α^* represent the dimensionless coordinate and the parameters scaled by the N_2 molecular diameter $\sigma = 0.36$ nm.

Fig. 3a shows gradual filling of this pore with CO_2 starting in the concave parts of the pore where the adsorption potential is significantly enhanced due to the surface curvature. The rest of the pore is filled at higher pressures. As a result, the average fluid density in the corrugated pores increases gradually and leads to the isotherms which are free from the layering transition effects that cause known artifacts observed in the results obtained by using standard NLDFT methods [39]. For N_2, we show only one density profile calculated at 10^{-7} relative pressure because the isotherm (Fig. 2) reaches the plateau and the densities above this pressures does not change significantly at this pressure. The fact that N_2 reaches a near maximum density in a 0.4 nm pore at 77 K may have significant practical meaning. The highly dense fluid in the ultramicropores is likely a reason for a very slow diffusion into these pores observed for ultramicroporous carbons like biochars[12].

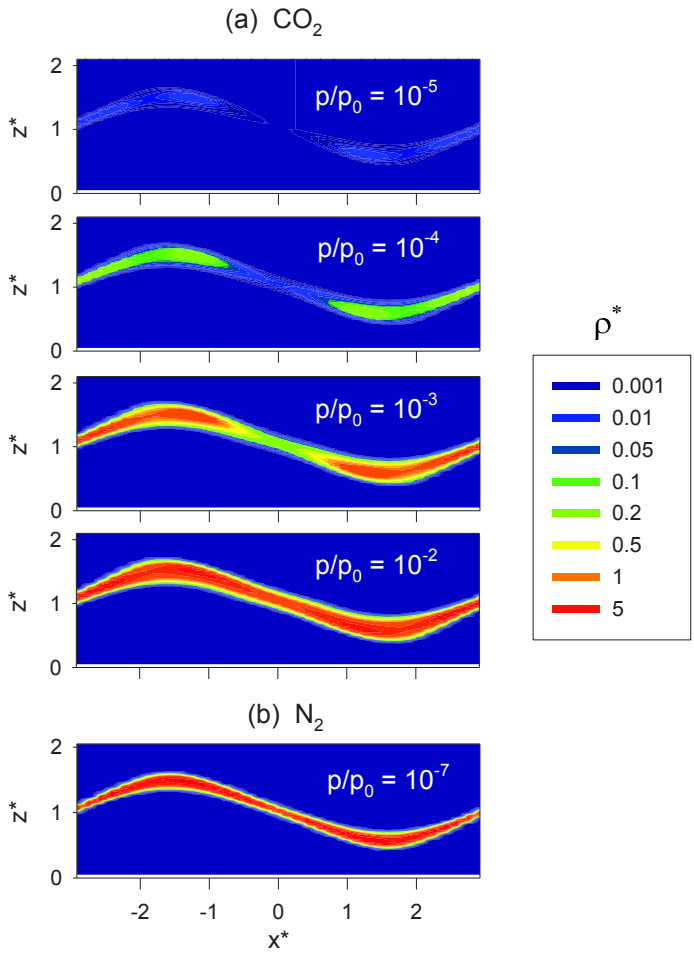

Fig. 3 – Density profiles of CO_2 (a) and N_2 (b) in the corrugated pore of width w = 0.4 nm calculated at increasing relative pressures.

3.2 Initial PSD analysis using 2D-NLDFT models

In the first step of our analysis, we assumed the lower pore width limit of both N_2 and CO_2 kernels to be w_{min} = 0.36 nm that is slightly wider than the molecular diameters of both gases. In figures 2 and 3 we present the differential PSDs and cumulative pore volumes calculated for C-CS and CH-CS carbon series. Three versions of the PSD and cumulative pore volume were calculated for each carbon sample. Two of them were obtained by fitting the relevant models to the individual N_2 and CO_2 adsorption isotherms. The third version is a result of the simultaneous (dual) fit [23] of these models to both isotherms.

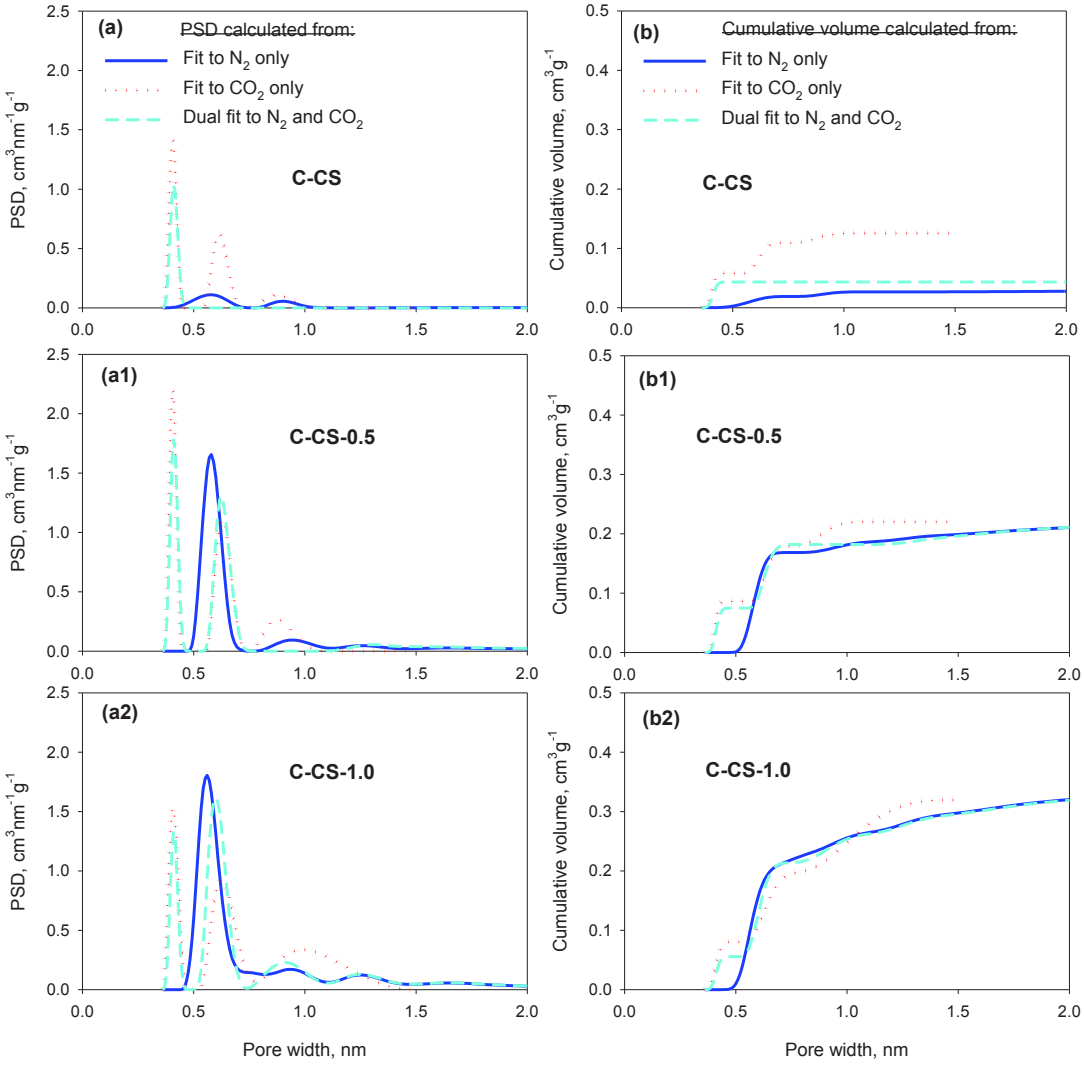

Fig. 4 – Differential PSDs (a) and cumulative pore volumes (b) of C-CS series of porous carbons calculated using 2D-NLDFT models (assuming w_{min} = 0.36 nm as the lowest pore width limit of both N_2 and CO_2 kernels).

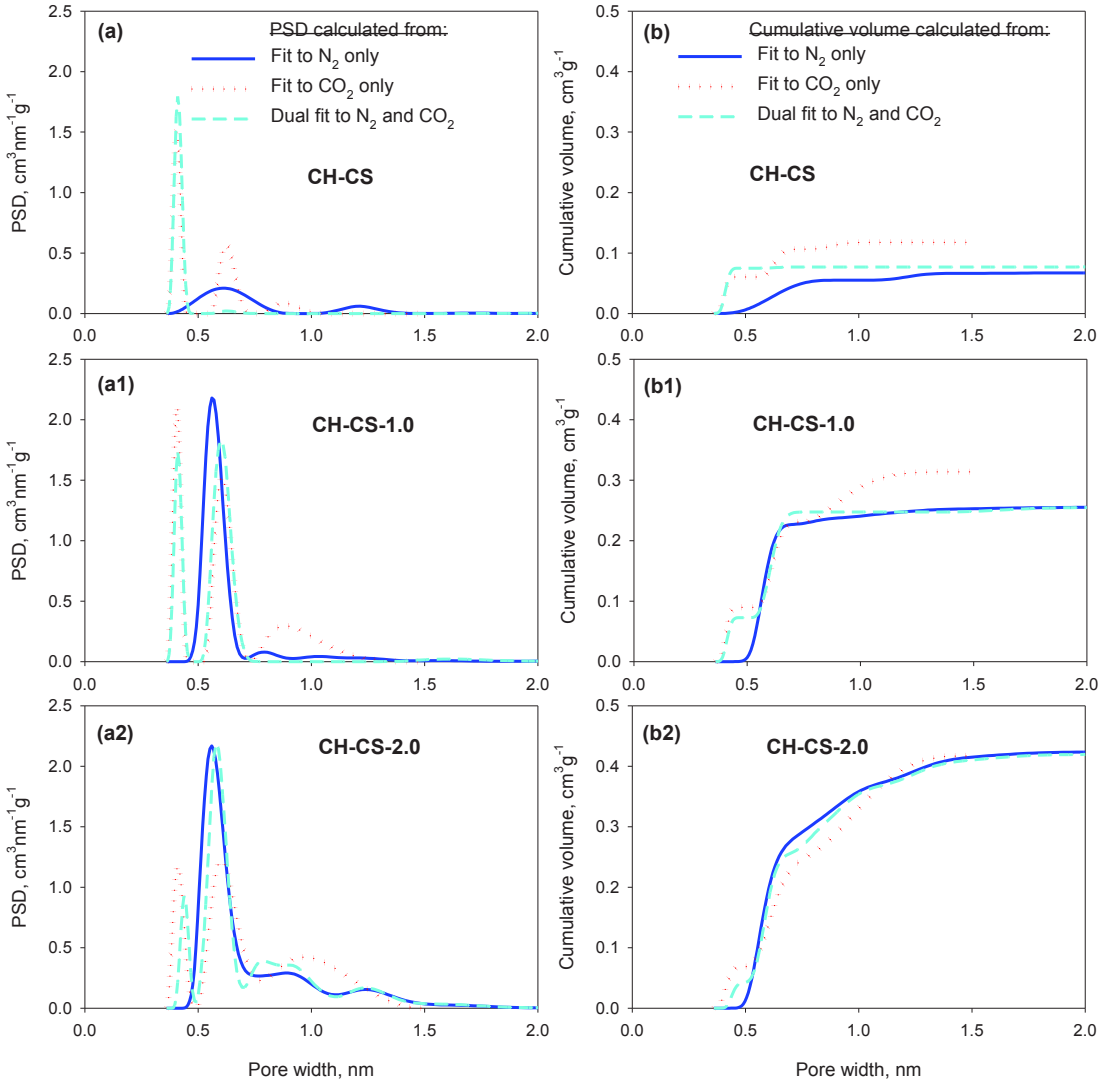

Fig. 5 – Same as Fig. 4 but for CH-CS series of porous carbons.

A general trend of increasing pore volumes upon activation is reflected by all differential PSDs and cumulative pore volumes of both series of carbons (Fig. 4 and 5). It is important, however, to note that the PSDs calculated from single N_2 isotherms do not show a peak at about 0.4 nm while this peak is present in all PSDs derived from CO_2 and dual models. The fact that the smallest pores of the studied carbons are detected by the CO_2 analysis at 273 K but not by N_2 at 77 K is consistent with earlier studies [15, 16] concluding that extremely slow diffusion of N_2 into very fine micropores at 77 K may significantly delay or restrict equilibration during adsorption process at low pressures.

It appears that CO_2 analysis may be a reasonable method for evaluating the PSD of ultramicropores, but we should keep in mind that, although we plotted the PSDs and pore

volumes up to 1.5 nm for this analysis, the upper limit of sensitivity for CO_2 analysis is in the range of 0.7-1.0 nm [37]. Therefore, the results of this analysis become increasingly uncertain for pores wider than 1.0 nm. This means that, in general, CO_2 analysis alone is not sufficient to describe the full range of PSD for any carbon, but when CO_2 isotherm crosses N_2, and the dual fit of N_2 is higher than single, like in the case of non-activated biochars such as C-CS and CH-Cs (Fig 4a and 4b), the CO_2 results should be considered more accurate than those of N_2.

Our PSD analysis also shows that the cumulative pore volumes derived from N_2 and the dual gas method (Fig. 4 and 5) merge above about 1 nm for all carbons except biochars C-CS and CH-CS, which suggests that the ultramicropores that initially were not filled by N_2 eventually fill up at higher pressures.

In Fig. 4, we present our results of fitting the NLDFT models to the experimental data in a way that may help to better understand the problem of slow diffusion affecting the N_2 adsorption analysis. All models show excellent fits to the single isotherms in this figure, but simultaneous fits of the models to two isotherms, in the dual analysis, deviate from the data in different extent, depending on the sample.

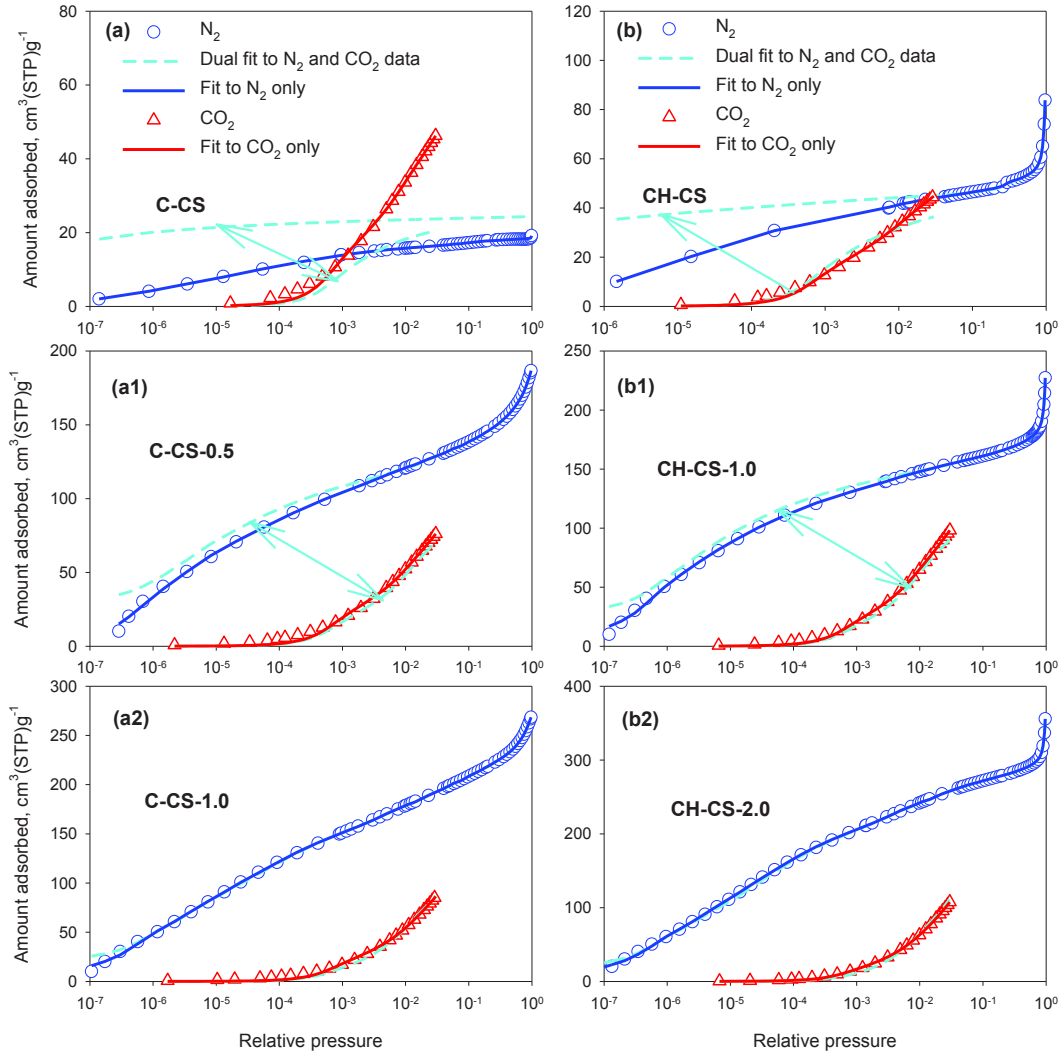

Fig. 6 – Single and dual model fits to the isotherms of N_2 and CO_2 for two series of porous carbons C-CS (a) and CH-CS (b) calculated using w_{min} = 0.36 nm.

The deviations of the fitted isotherms from the data are the highest for biochar samples C-CS and CH-CS (Fig. 6a and 6b) where the fits to N_2 isotherms are far above the experimental data points in the low-pressure region for both samples. At higher relative pressures, the N_2 fit improves for CH-CS (Fig. 6b) but remains above the data in the whole pressure range for C-CS sample (Fig. 6a). The upward deviations of N_2 fits are balanced by the downward deviations of CO_2 fits at higher relative pressures for both biochars. To explain these systematic deviations, we need to realize that the fits to the two isotherms are mathematically interrelated via the underlying NLDFT models and the calculated PSDs. This means that the N_2 isotherm influences the fit of CO_2 and vice versa. In the case of biochars, the values of the differential PSDs (Fig. 4a and 5a) and cumulative volumes (Fig. 4b, and 5b) obtained from

CO_2 are higher than those obtained from N_2. As a result, the predicted (fitted) N_2 isotherms are influenced by the experimental ones of CO_2 and are statistically forced to be higher than the experimental ones. This, and the opposite effect on the predicted CO_2 isotherms are pointed out by arrows in Fig. 6. As the CO_2 activation progresses, the simultaneous fit of the 2D-NLDFT models to both experimental isotherms significantly improves for both carbon series. Some small upwards deviations from the N_2 data are still observed for C-CS-0.5 and CH-CS-1.0 shown in Fig. 6a1 and 6b1, but these deviations practically disappear for the ACs with the most developed pore structure: C-CS-1.0 and CH-CS-2.0 (Fig. 6a2 and 6b2).

3.3 Refinement of the PSD analysis

To refine our approach and resolve the existing inconsistency between the results obtained from N_2 and CO_2 analysis of biochars, we look more closely into the fitting procedure used in the dual gas method. It is important to understand that both kernels predict corresponding isotherms based on the common PSD obtained from the simultaneous fit of the corresponding kernels to these isotherms. When the experimental isotherm of N_2 is underestimated at low-pressure range due to a slow diffusion into narrow pores, it means that these pores physically do not contribute to this isotherm, but their theoretical adsorption amount is predicted by the N_2 kernel. This causes the discrepancy between measured and calculated N_2 isotherms. It follows that, in order to improve the agreement between these isotherms, some theoretical isotherms for narrow pores should be excluded from the N_2 kernel. A similar approach [40] was applied in the PSD analysis of hierarchical zeolites using argon adsorption and mercury intrusion in which the theoretical kernels were zero padded outside the common pore size range where both methods probe the porosity.

To test this hypothesis, we increased the lower pore width limit of the N_2 kernel from the initial w_{min} = 0.36 nm to slightly higher values, and we found that with w_{min} = 0.5 nm we obtained an excellent dual fit to both N_2 and CO_2 isotherms for biochars (Fig. 7a and 7b). Pore width of 0.5 nm appears to be a reasonable limit of N_2 accessibility to ultra micropores of non-activated biochars at low pressures and cryogenic temperatures. For activated carbons, a very good fit was obtained (Fig. 7) using decreasing w_{min} values with the increasing extent of activation. This trend may be explained by the fact that activation with CO_2 widens the pores and removes constrictions blocking access to the narrowest pores.

The value of the lower pore width limit w_{min} for the N_2 kernel should not only be regarded as an additional parameter that is derived from the fitting procedure of N_2 and CO_2 isotherms. It also has a physical meaning of an estimate of the minimum pore width accessible to N_2

molecules at the measurement conditions. In the dual gas analysis of carbons that are not extremely ultramicroporous the default value of this parameter w_{min} = 0.36 nm gives a good fit of the model to the data [23]. For the ultramicroporous carbons like the biochars studied in this work, the additional adjustment/fitting of this parameter appears to be necessary to obtain a good agreement between the model and the data.

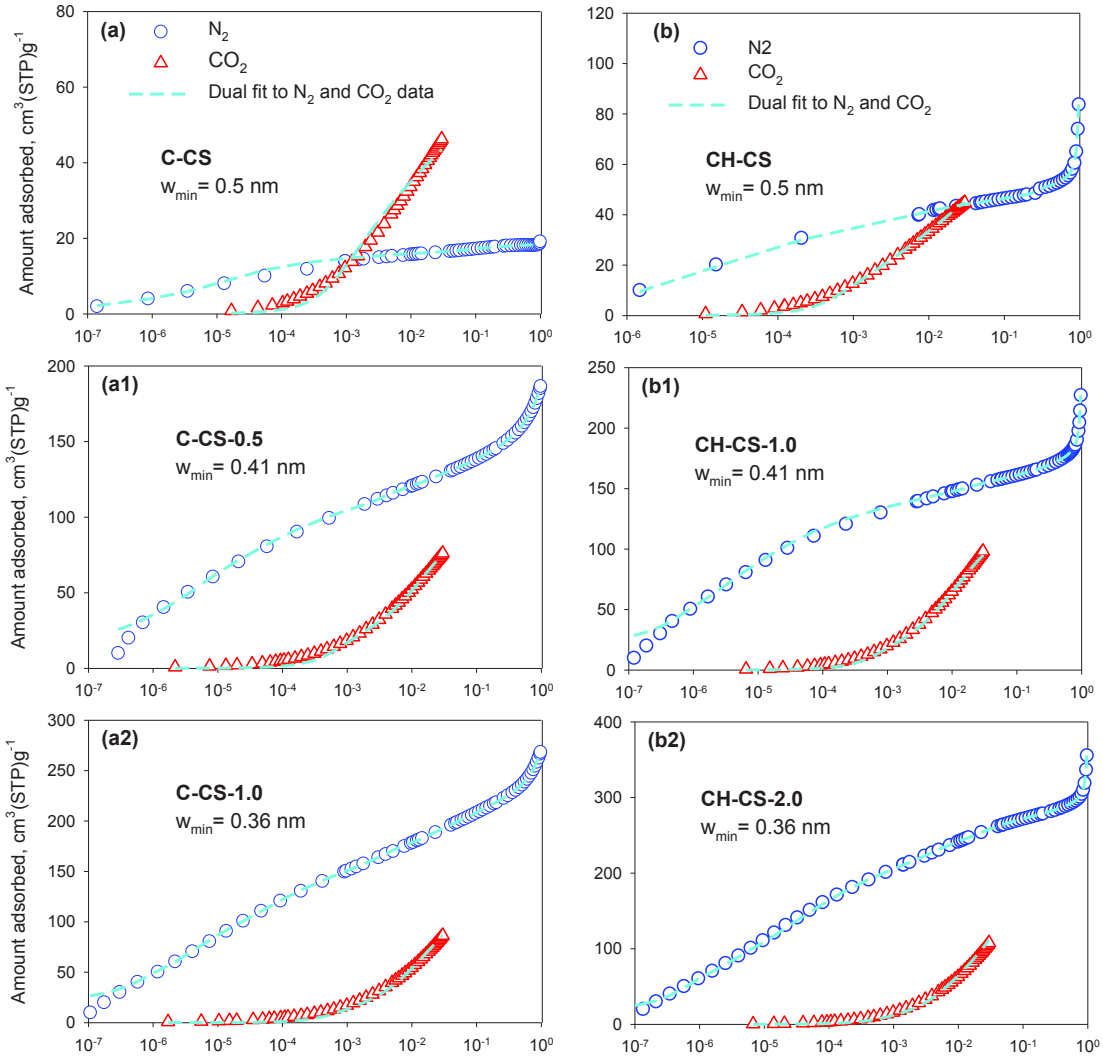

Fig. 7 – Same as Fig. 6 but using variable lower pore width limit w_{min} of the N_2 kernel.

Based on the excellent agreement of the dual model with experimental data of both gases, we chose this model as the most accurate and comprehensive method of the pore structure analysis of our biochars and activated carbons. Using this model and the pore width limits w_{min} listed in Table 2, we calculated the PSDs and cumulative pore volumes of all samples (Fig. 8 and 9). Table 2 also contains selected structural characteristics of all samples derived

from the 2D-NLDFT analysis which include specific surface area, S_{Dual}, obtained from the dual gas method and cumulative pore volumes calculated at different pore widths using the dual gas method and single isotherms. Pore volumes are denoted as $V_{w,Dual}$, $V_{w,\ N2}$, $V_{w,\ CO2}$, where w represents the pore width at which the volume was calculated.

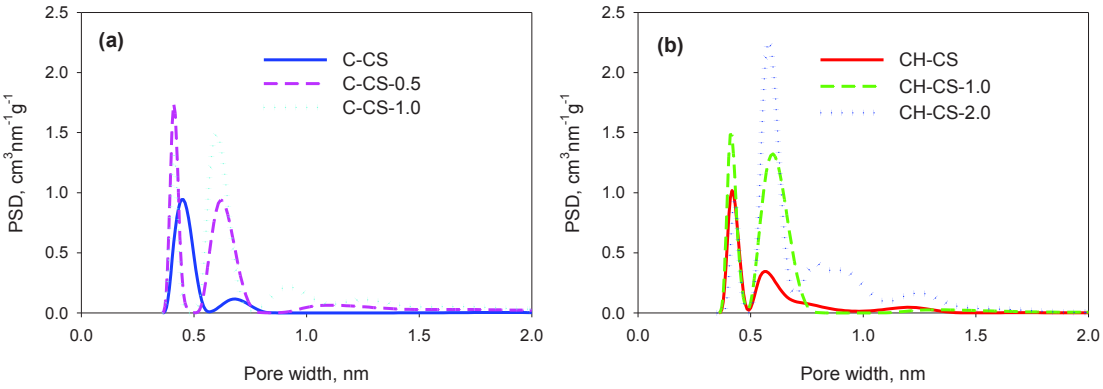

Fig. 8 – Differential PSDs of C-CS (a) and CH-CS (b) series of porous carbons calculated using dual gas method and 2D-NLDFT models.

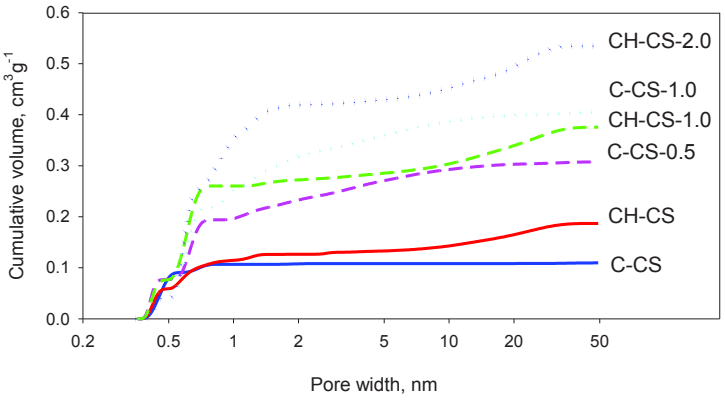

Fig. 9- Cumulative pore volumes of C-CS and CH-CS series of samples calculated using the same method as in Fig. 8.

The PSDs and cumulative pore volumes calculated for samples that received similar treatment are similar for both series of carbons. The main difference is that C-CS samples show a plateau of the cumulative pore volumes (Fig. 9) in the range of larger mesopores between 15 and 50 nm while CH-CS samples show an increase in this range.

Table 2. Structural characteristics of C-CS and CH-CS carbons obtained from the 2D-NLDFT analysis.

Sample	S_{Dual} (m^2g^{-1})	$V_{0.5\ nm,\ N2}$ (cm^3g^{-1})	$V_{0.5\ nm,\ Dual}$ (cm^3g^{-1})	$V_{1.5\ nm\ CO2}$ (cm^3g^{-1})	$V_{1.5\ nm,\ Dual}$ (cm^3g^{-1})	$V_{50\ nm,\ N2}$ (cm^3g^{-1})	$V_{50\ nm,\ Dual}$ (cm^3g^{-1})	w_{min} (nm)
C-CS	450	0.0	0.08	0.12	0.10	0.03	0.11	5.0
C-CS-0.5	840	0.0	0.08	0.22	0.22	0.28	0.31	4.1
C-CS-1.0	1010	0.0	0.05	0.32	0.29	0.40	0.41	3.6
CH-CS	490	0.0	0.06	0.12	0.12	0.12	0.19	5.0
CH-CS-1.0	1010	0.01	0.08	0.31	0.27	0.36	0.37	4.1
CH-CS-2.0	1280	0.01	0.04	0.42	0.41	0.54	0.54	3.6

The fact that CO_2 isotherm in the dual analysis provides the most accurate information about narrow micropores suggests that this isotherm may be combined with N_2 isotherm measured for the relative pressures starting at p/p_0 about 0.001 rather than at 10^{-6}, which would save the time of the N_2 analysis. To demonstrate the feasibility of such an approach we used as an example N_2 isotherm measured on C-CS-0.5 sample truncated below 0.001 p/p_0 in combination with full CO_2 isotherm. The dual analysis shows an excellent fit to shortened N_2 and full CO_2 isotherms (Fig. 10a). The PSD calculated for this set of data agrees very well with that derived from full isotherms (Fig. 10b).

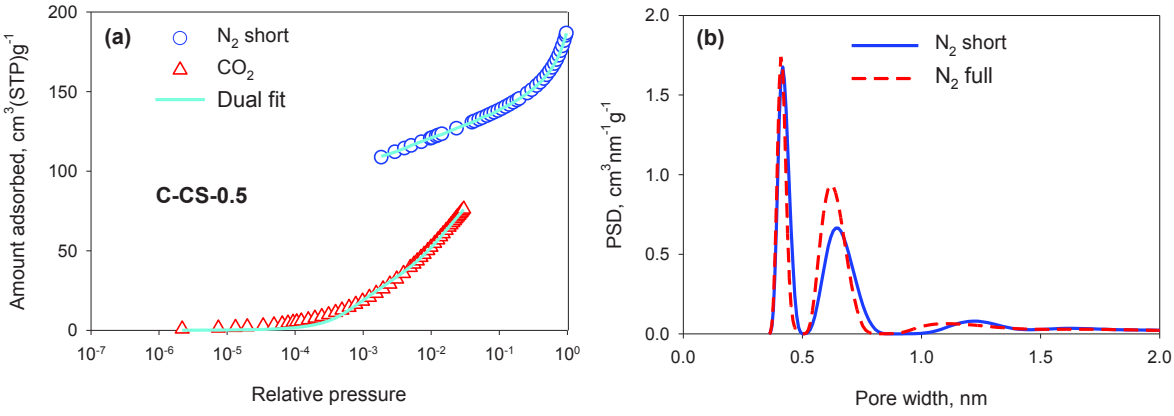

Fig. 10- Dual method analysis of truncated (short) N_2 and full CO_2 isotherms of C-CS-0.5 sample. (a) Fit of both isotherms. (b) Comparison of PSDs derived from the isotherms shown in Fig 10a and full isotherms shown in Fig. 7a1 (w_{min} = 0.41nm)

4. Conclusions

In this study, we presented a novel approach to addressing a very difficult to characterize materials which are known as chars, biochars and ultramicroporous carbons. We undoubtedly showed that the dual gas analysis of the N_2 and CO_2 adsorption isotherms provides more detailed comprehensive information about the pore microstructure of biochars and activated carbons than single N_2 isotherms. The PSDs of our microporous carbon samples calculated by the simultaneous fit of the 2D-NLDFT models to N_2 and CO_2 isotherms showed a peak at about 0.4 nm, which was also detected by CO_2 but not by the single N_2 analysis. This fact is related to the extremely slow diffusion that may significantly delay or restrict access of N_2 into very narrow micropores at cryogenic temperatures and low pressures. Additional information was obtained from the cumulative pore volumes. Cumulative pore volumes derived from the dual method and single N_2 isotherm merged above about 1 nm for all carbons except for biochars, indicating that ultramicropores that were not initially filled by N_2 at low pressures eventually filled up at higher pressures of the measurement.

In the new approach introduced in this study, the lower pore width limit w_{min} of the N_2 kernel is treated as an adjustable parameter. The value of w_{min} has a physical meaning as it provides an estimate of the minimum pore width accessible to N_2 molecules at the measurement conditions. By modifying this parameter, we dramatically improved the quality of fit of the dual model to both isotherms measured on the non-activated biochars and mildly activated carbons. This modification was based on the observed interrelation between simultaneously fitted CO_2 and N_2 isotherms. An excellent fit of the dual model to both N_2 and CO_2 isotherms for all studied samples, demonstrates that this method is reliable and robust.

Finally, since CO_2 isotherm in the dual analysis provides the most accurate information about narrow micropores, this isotherm may be combined with N_2 isotherm measured for the relative pressures starting at p/p_0 about 0.001 rather than at 10^{-6}, which would save the time of the N_2 analysis.

This study may become a reference for the correct textural characterization of biochars and carbon materials with an important fraction of porosity narrower than 0.7 nm.

Acknowledgments

We are thankful to Ms. Fatma Mbarki and M. Taher Selmi for preparing the materials characterized in this study.

References

[1] C.J. Atkinson, J.D. Fitzgerald, N.A. Hipps, Potential mechanisms for achieving agricultural benefits from biochar application to temperate soils: a review, Plant and Soil 337 (2010) 1-18.
[2] J. Lehmann, M.C. Rillig, J. Thies, C.A. Masiello, W.C. Hockaday, D. Crowley, Biochar effects on soil biota – A review, Soil Biology and Biochemistry 43 (2011) 1812-1836.
[3] J.-H. Park, Y.S. Ok, S.-H. Kim, J.-S. Cho, J.-S. Heo, R.D. Delaune, D.-C. Seo, Competitive adsorption of heavy metals onto sesame straw biochar in aqueous solutions, Chemosphere 142 (2016) 77-83.
[4] H. Lu, W. Zhang, Y. Yang, X. Huang, S. Wang, R. Qiu, Relative distribution of Pb2+ sorption mechanisms by sludge-derived biochar, Water research 46 (2012) 854-862.
[5] D. Kolodynska, J. Bak, M. Koziol, L.V. Pylychuk, Investigations of Heavy Metal Ion Sorption Using Nanocomposites of Iron-Modified Biochar, Nanoscale Res Lett 12 (2017) 433.
[6] M. Inyang, E. Dickenson, The potential role of biochar in the removal of organic and microbial contaminants from potable and reuse water: a review, Chemosphere 134 (2015) 232-240.
[7] R.-k. Xu, S.-c. Xiao, J.-h. Yuan, A.-z. Zhao, Adsorption of methyl violet from aqueous solutions by the biochars derived from crop residues, Bioresource technology 102 (2011) 10293-10298.
[8] C. Chen, W. Zhou, D. Lin, Sorption characteristics of N-nitrosodimethylamine onto biochar from aqueous solution, Bioresource technology 179 (2015) 359-366.
[9] R.P. Overend, E. Chornet, Fractionation of lignocellulosics by steam-aqueous pretreatments, Phil. Trans. R. Soc. Lond. A 321 (1987) 523-536.
[10] A.M. Borrero-López, E. Masson, A. Celzard, V. Fierro, Modelling the reactions of cellulose, hemicellulose and lignin submitted to hydrothermal treatment, Industrial Crops and Products 124 (2018) 919-930.
[11] B. Hu, K. Wang, L. Wu, S.H. Yu, M. Antonietti, M.M. Titirici, Engineering carbon materials from the hydrothermal carbonization process of biomass, Advanced Materials 22 (2010) 813-828.
[12] A.M. Borrero-López, V. Fierro, A. Jeder, A. Ouederni, E. Masson, A. Celzard, High added-value products from the hydrothermal carbonisation of olive stones, Environmental Science and Pollution Research 24 (2017) 9859-9869.
[13] A. Jeder, A. Sanchez-Sanchez, P. Gadonneix, E. Masson, A. Ouederni, A. Celzard, V. Fierro, The severity factor as a useful tool for producing hydrochars and derived carbon materials, Environmental Science and Pollution Research 25 (2018) 1497-1507.
[14] T. Selmi, A. Sanchez-Sanchez, P. Gadonneix, J. Jagiello, M. Seffen, H. Sammouda, A. Celzard, V. Fierro, Tetracycline removal with activated carbons produced by hydrothermal carbonisation of Agave americana fibres and mimosa tannin, Industrial Crops and Products 115 (2018) 146-157.
[15] F. Rodríguez-Reinoso, J.d.D. López-González, C. Berenguer, Activated carbons from almond shells—II: Characterization of the pore structure, Carbon 22 (1984) 13-18.
[16] F. Rodriguez-Reinoso, J.d.D. Lopez-Gonzalez, C. Berenguer, Activated carbons from almond shells—I: Preparation and characterization by nitrogen adsorption, Carbon 20 (1982) 513-518.
[17] J. Garrido, A. Linares-Solano, J.M. Martin-Martinez, M. Molina-Sabio, F. Rodriguez-Reinoso, R. Torregrosa, Use of nitrogen vs. carbon dioxide in the characterization of activated carbons, Langmuir : the ACS journal of surfaces and colloids 3 (1987) 76-81.
[18] D. Lozano-Castelló, D. Cazorla-Amorós, A. Linares-Solano, Usefulness of CO2 adsorption at 273 K for the characterization of porous carbons, Carbon 42 (2004) 1233-1242.

[19] S. Schaefer, V. Fierro, M.T. Izquierdo, A. Celzard, Assessment of hydrogen storage in activated carbons produced from hydrothermally treated organic materials, International Journal of Hydrogen Energy 41 (2016) 12146-12156.
[20] S. Schaefer, V. Fierro, A. Szczurek, M.T. Izquierdo, A. Celzard, Physisorption, chemisorption and spill-over contributions to hydrogen storage, International Journal of Hydrogen Energy 41 (2016) 17442-17452.
[21] H. McLaughlin, F. Shields, J. Jagiello, G. Thiele, Analytical options for biochar adsorption and surface area, North American Biochar Conference, Sonoma, CA, 2012.
[22] M.M. Dubinin, The Potential Theory of Adsorption of Gases and Vapors for Adsorbents with Energetically Nonuniform Surfaces, Chemical Reviews 60 (1960) 235-241.
[23] J. Jagiello, C. Ania, J.B. Parra, C. Cook, Dual gas analysis of microporous carbons using 2D-NLDFT heterogeneous surface model and combined adsorption data of N2 and CO2, Carbon 91 (2015) 330-337.
[24] J. Jagiello, C.O. Ania, J.B. Parra, L. Jagiello, J.J. Pis, Using DFT analysis of adsorption data of multiple gases including H2 for the comprehensive characterization of microporous carbons, Carbon 45 (2007) 1066-1071.
[25] J. Jagiello, W. Betz, Characterization of pore structure of carbon molecular sieves using DFT analysis of Ar and H2 adsorption data, Microporous and Mesoporous Materials 108 (2008) 117-122.
[26] J. Jagiello, J.P. Olivier, 2D-NLDFT adsorption models for carbon slit-shaped pores with surface energetical heterogeneity and geometrical corrugation, Carbon 55 (2013) 70-80.
[27] J. Jagiello, J.P. Olivier, Carbon slit pore model incorporating surface energetical heterogeneity and geometrical corrugation, Adsorption 19 (2013) 777-783.
[28] P. Kleszyk, P. Ratajczak, P. Skowron, J. Jagiello, Q. Abbas, E. Frąckowiak, F. Béguin, Carbons with narrow pore size distribution prepared by simultaneous carbonization and self-activation of tobacco stems and their application to supercapacitors, Carbon 81 (2015) 148-157.
[29] G. Gregis, J.-B. Sanchez, S. Schaefer, V. Fierro, F. Berger, I. Bezverkhyy, G. Weber, J.-P. Bellat, A. Celzard, Detection of lung cancer bio-markers in human breath using a micro-fabricated air analyzer, Materials Today: Proceedings 2 (2015) 4664-4670.
[30] G. Gregis, S. Schaefer, J.-B. Sanchez, V. Fierro, F. Berger, I. Bezverkhyy, G. Weber, J.-P. Bellat, A. Celzard, Characterization of materials toward toluene traces detection for air quality monitoring and lung cancer diagnosis, Materials Chemistry and Physics 192 (2017) 374-382.
[31] F. Mbarki, A. Kesraoui, M. Seffen, P. Ayrault, Kinetic, Thermodynamic, and Adsorption Behavior of Cationic and Anionic Dyes onto Corn Stigmata: Nonlinear and Stochastic Analyses, Water, Air, & Soil Pollution 229 (2018) 95.
[32] F.L. Braghiroli, V. Fierro, M.T. Izquierdo, J. Parmentier, A. Pizzi, A. Celzard, Kinetics of the hydrothermal treatment of tannin for producing carbonaceous microspheres, Bioresource Technology 151 (2014) 271-277.
[33] J. Illingworth, P.T. Williams, B. Rand, Characterisation of biochar porosity from pyrolysis of biomass flax fibre, Journal of the Energy Institute 86 (2013) 63-70.
[34] J. Jagiello, Stable numerical solution of the adsorption integral equation using splines, Langmuir : the ACS journal of surfaces and colloids 10 (1994) 2778-2785.
[35] M. Lopez-Ramon, J. Jagiello, T. Bandosz, N. Seaton, Determination of the pore size distribution and network connectivity in microporous solids by adsorption measurements and Monte Carlo simulation, Langmuir : the ACS journal of surfaces and colloids 13 (1997) 4435-4445.
[36] M. Seredych, J. Jagiello, T.J. Bandosz, Complexity of CO2 adsorption on nanoporous sulfur-doped carbons – Is surface chemistry an important factor?, Carbon 74 (2014) 207-217.
[37] P.I. Ravikovitch, A. Vishnyakov, R. Russo, A.V. Neimark, Unified Approach to Pore Size Characterization of Microporous Carbonaceous Materials from N2, Ar, and CO2 Adsorption Isotherms†, Langmuir : the ACS journal of surfaces and colloids 16 (2000) 2311-2320.
[38] J. Jagiello, M. Thommes, Comparison of DFT characterization methods based on N2, Ar, CO2, and H2 adsorption applied to carbons with various pore size distributions, Carbon 42 (2004) 1227-1232.

[39] A.V. Neimark, Y. Lin, P.I. Ravikovitch, M. Thommes, Quenched solid density functional theory and pore size analysis of micro-mesoporous carbons, Carbon 47 (2009) 1617-1628.
[40] J. Kenvin, J. Jagiello, S. Mitchell, J. Perez-Ramirez, Unified method for the total pore volume and pore size distribution of hierarchical zeolites from argon adsorption and mercury intrusion, Langmuir : the ACS journal of surfaces and colloids 31 (2015) 1242-1247.

***Graphical Abstract**

Graphical abstract